Electromagnetic scattering from a plasma coated perfect electromagnetic conductor cylinder placed in chiral metamaterials

M. Z. YAQOOB[a,*], A. GHAFFAR[b], I. SHAKIR[c], M. Y. NAZ[d], S. AHMED[e], Q. A. NAQVI[f]
[a]*Department of Physics, G.C. University, Faisalabad, Pakistan*
[b,d]*Department of Physics, University of Agriculture, Faisalabad, Pakistan*
[c]*Department of Electrical Engineering, King Saud University, Saudi Arabia*
[e,f]*Department of Electronics, Quaid-i-Azam University, Islamabad, Pakistan*

Electromagnetic scattering from an anisotropic plasma coated PEMC cylinder placed in isotropic chiral media is investigated. The PEMC cylinder is concentrically coated with an anisotropic plasma, the medium hosting the coated cylinder is also considered as chiral or chiral-nihility metamaterial. The fields are expanded in terms of two dimensional cylindrical wave vector functions to find out the solution for the fields scattered from the concentric PEMC circular cylinders and an anisotropic plasma circular cylinders immersed in chiral metamaterial. Coated perfect electric conductor (PEC)/perfect magnetic conductor (PMC) are obtained by taking the scalar admittance parameter $M \rightarrow \pm\infty$ and $M = 0$ of the inner PEMC cylinder. It is concluded that (RCS) scattering from different coated perfect cylinders can be controlled by proper choice of host medium as well as the type of the cylinder. The comparisons of the numerically computed results of the presented formulations with the published results of some special cases confirm the accuracy of the presented analysis.

(Received May 1, 2014; accepted May 15, 2014)

Keywords: Scattering, Plasma, Perfect Electromagnetic Conductor, Chiral, Cylinder

1. Introduction

In recent years, chiral materials have attained a lot of attention because that the negative refractive index can be realized in the chiral metamaterials [1]. These materials may exhibit exceptional electromagnetic response that does not occur in natural materials. It has been found that materials with complex properties can find more probable applications in the microwave and optical regions. There are many types of metamaterials have been found like chiral/achiral, pseudochiral, chiral nihility materials, plasma, chiroplasma, anisotropic, bi-anisotropic, inhomogeneous, uniaxial, double-positive(DPS), double negative(DNG), epsilon-negative(ENG) and mu-negative (MNG) meta-materials and many more. These materials may have potential applications in optical signal processing, radar cross section control, optical fibers, special radar absorber materials, and in high performance microstrip antenna design [2-6].

The extraordinary electromagnetic properties of these materials have magnetized many scientists and engineers for further study and research, like chiral metamaterial is an optically active material which is made up of microscopic continuous objects and has ability to circularly polarize the incident plane polarized light [7]. Extensive work has been done on the propagation, scattering and transmission of electromagnetic waves through the chiral material. Bassari et al. analyzed the behavior of electromagnetic radiation at chiral-dielectric interface as well as through the chiral slab and determine the Brewster angle [8]. Furthermore scattering problems related to chiral, chiral coated objects is the main interest of many researchers and engineers due to their stealth capability. Kanhal et al discussed the electromagnetic scattering from chiral cylinder having arbitrary cross section [9] and now his work is extended to scattering problem i.e., scattering of electromagnetic radiation from a chiral cylinder placed in chiral metamaterial [10]. Jaggaard et al examined the scattering of electromagnetic radiation from circular structures coated with the chiral medium and reported the possible effects and applications of chiral coated geometries [11]. Ahmad et al studied the problem of scattering from chiral coated nihility cylinder [12]. Recently, Sobia et al extended the Ahmad's work and placed the chiral coated nihility cylinder in chiral metamaterial and analyzed the scattered fields from different coated cylinders as well as the host mediums i.e., free space/ Achiral material, chiral and chiral nihility [13].

Moreover, in parallel to chiral metamaterial, plasma coated conducting geometries also stimulated many researchers due to their scattering amplitude reducing ability and practical uses in the field of aerospace sciences and defense technology [14-15]. Plasma is a quasi-neutral mixture of charged and neutral particles which exhibits a highly ionized state of a gas. When the space objects like missiles and satellites having cylindrical and spherical geometries respectively, come into atmosphere, they immerse into ionosphere and can be modeled as plasma coated conducting cylinder/ sphere. Cheng et al discussed the geometry for electromagnetic scattering from anisotropic plasma coated perfect electric conductor (PEC) cylinder [16]. You Bin et al discussed the more complicated case of scattering than Cheng, in which the PEC cylinder is not at the center of plasma coating i.e., eccentric plasma coated PEC cylinder and reported that the scattering amplitude is sensitive to the distance of cylinder from center as well as the plasma parameters i.e., plasma density and collision frequency [17]. Recently a more general and more complicated scattering problem i.e., electromagnetic scattering from anisotropic plasma coated prefect electromagnetic conductor (PEMC) cylinder has been discussed and reported that PEMC helps to reduce the radar cross section (RCS) [18]. PEMC materials has been attracted by many scientist and researchers due to its potential and tremendous applications in the field of communication, optical sensing and defense technology. PEMC is the more general form of perfect conductors i.e., perfect electric conductor PEC and perfect magnetic conductor PMC [19-25].

In this research work, scattering from homogenous anisotropic plasma coated PEMC cylinder placed in chiral metamaterial is discussed. The present theory of scattering is general for following scattering problems under special conditions, which shows the novelty of our work i.e., from a simple formulation the subsequent scattering problems can be formulated.

- Isotropic plasma coated perfect conductor (PEC, PMC and PEMC) cylinders placed in achiral/ chiral/ chiral nihility metamaterial.
- Metamaterial coated perfect conductor (PEC, PMC and PEMC) cylinders placed in achiral/ chiral/ chiral nihility metamaterial.
- Anisotropic/ isotropic plasma cylinder placed in achiral/ chiral/ chiral nihility metamaterial.
- Metamaterial cylinder placed in achiral/ chiral/ chiral nihility metamaterial.
- Perfect conductor (PEC, PMC and PEMC) cylinders placed in achiral/ chiral/ chiral nihility metamaterial.

In the whole study the time harmonics $e^{-j\omega t}$ is taken and suppressed for all fields. The study is organized as: section 2 presents the analytical formulation of scattering problem where the section 3 and 4 contain the numerical results, their discussion and conclusion respectively.

2. Analytical formulations

The whole space is divided into three regions as depicted in Fig. 1. The region I is termed as chiral metamaterial in which the anisotropic plasma coated PEMC cylinder is placed. The homogenous anisotropic plasma coating is termed as region II and the PEMC cylinder is termed as region III. The PEMC cylinder is taken as infinite, concentrically coated with anisotropic plasma material and placed along z-axis of coordinate system. The electromagnetic properties of each material in each region is describe below as

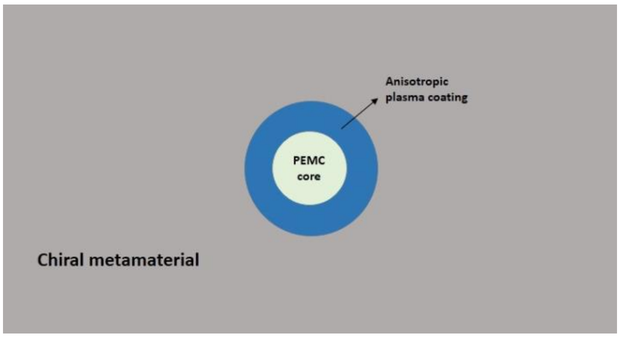

Fig. 1. Anisotropic plasma coated PEMC cylinder placed in chiral metamaterial.

2.1 Chiral metamaterial

The region I represents the infinite homogenous, isotropic and reciprocal chiral metamaterial. The constitutive relations for such class of chiral metamaterial are given as [7,10]

$$\vec{D} = \varepsilon_c \vec{E} - j\beta \sqrt{\varepsilon_0 \mu_0}\, \vec{H} \quad (1)$$

$$\vec{B} = \mu_c \vec{H} + j\beta \sqrt{\varepsilon_0 \mu_0}\, \vec{E} \quad (2)$$

where ε_c, μ_c and β are the permittivity, permeability and chirality parameter of chiral material respectively. The wave numbers which satisfy the above constitutive relations and wave equation are given as

$$k_{\pm} = \omega\left(\sqrt{\varepsilon_c \mu_c} \pm \beta\right) \quad (3)$$

here k_+ and k_- stands for right circularly polarize wave (RCP) and left circularly polarize wave (LCP) respectively. The chiral metamaterial transforms into the chiral nihility material by imposing the nihility conditions i.e., $\varepsilon_c \to 0, \mu_c \to 0$ [12-13] and the above constitutive relations alter in to the following form

$$\vec{D} = -j\beta \sqrt{\varepsilon_0 \mu_0}\, \vec{H} \quad (4)$$

$$\vec{B} = j\beta \sqrt{\varepsilon_0 \mu_0}\, \vec{E} \quad (5)$$

$$k_{\pm} = \omega(\pm \beta) \quad (6)$$

where the impedance for chiral material and chiral nihility material is $\eta_1 = \sqrt{\frac{\mu_c}{\varepsilon_c}}$ and $\eta_0 = \sqrt{\frac{\mu_0}{\varepsilon_0}}$ respectively.

2.2. Anisotropic plasma coating

The region 2 represents the homogenous anisotropic plasma material coating. When the isotropic and homogeneous plasma material comes under the influence of external magnetic field then it's becomes the anisotropic material and its electromagnetic properties are characterized by the following relative permittivity tensor as [18]

$$[\varepsilon] = \begin{bmatrix} \varepsilon_1 & \varepsilon_2 & 0 \\ -\varepsilon_2 & \varepsilon_1 & 0 \\ 0 & 0 & \varepsilon_3 \end{bmatrix} \tag{7}$$

where the elements of this relative permittivity tensor $\varepsilon_1, \varepsilon_2$and ε_3 are the function of electron density, plasma frequency, collision frequency of plasma species and the external magnetic field strength. Their explicit expressions are found in literature extensively as [14-16]. The wavenumbers in anisotropic plasma for transverse magnetic (TM) polarization and transverse electric (TE) polarization are $k_1 = \frac{k_0}{\sqrt{m}}$, and $k_2 = \frac{k_0}{\sqrt{m_3}}$ respectively, where $= \frac{\varepsilon_1}{{\varepsilon_1}^2+{\varepsilon_2}^2}$, $m_3 = \frac{1}{\varepsilon_3}$, $k_0 = \omega\sqrt{\varepsilon_0\mu_0}$, impedance of the plasma material is $\eta = \sqrt{\frac{m\mu_0}{\varepsilon_0}}$. [16,18].

2.3. PEMC cylinder

The infinitely long circular PEMC cylinder is represented by the region III in this geometry. The PEMC is the generalize form of PEC and PMC as discussed above. It reflects all electromagnetic radiations regardless of their frequencies, due to this reason it is considered as perfect reflector or perfect boundary for electromagnetic radiations [20]. It characterized by the scalar admittance parameter *M*. For $M = 0$ and $M \rightarrow \pm\infty$ PEMC turns into the PMC and PEC respectively and its boundary mathematically modeled as [19]

$$\left.\begin{aligned} \hat{n} \times \left(\vec{H} + M\vec{E}\right) = 0 \\ \hat{n} \cdot \left(\vec{D} - M\vec{B}\right) = 0 \end{aligned}\right\} \tag{8}$$

In above, $\hat{n}$ is the unit normal and M is the scalar admittance parameter.

2.4 Cylindrical wave excitation:

The fields are expanded in terms of cylindrical wave vector functions (CWFs) for the sake of convenience and symmetry as given in [10]

$$\boldsymbol{N}_n^p(k\rho) = \hat{\boldsymbol{z}} Z_n^{(p)}(k\rho)e^{jn\varphi} \tag{9}$$

$$\boldsymbol{M}_n^{(p)}(k\rho) = \hat{\boldsymbol{\rho}}\left(\frac{in}{k\rho}\right) Z_n^{(p)}(k\rho)e^{jn\varphi} - \hat{\boldsymbol{\varphi}} Z'^{(p)}_n(k\rho)e^{jn\varphi} \tag{10}$$

where for p = 1, 2, and 3 the radial function $Z_n^{(p)}(k\rho)$ transform into the Bessel function of first kind, Hankel function of first and second kind respectively. In above, the wave number k will transform into the k_+ and k_- for RCP and LCP wave respectively in chiral medium. The chiral metamaterial supports the circularly polarized waves therefore the incident field may be the right circularly polarized (RCP) or the left circularly polarized (LCP). Consider first the incident field is the RCP and given below as [10, 13]

$$\vec{E}^i = \sum_{n=-\infty}^{\infty} j^{-n}\left[\boldsymbol{M}_n^{(1)}(k_+\rho) + \boldsymbol{N}_n^{(1)}(k_+\rho)\right] \tag{11}$$

$$\vec{H}^i = \frac{j}{\eta}\sum_{n=-\infty}^{\infty} j^{-n}\left[\boldsymbol{M}_n^{(1)}(k_+\rho) + \boldsymbol{N}_n^{(1)}(k_+\rho)\right] \tag{12}$$

The scattered fields are given as

$$\vec{E}^s = \sum_{n=-\infty}^{\infty} j^n \left[a_n\left[\boldsymbol{M}_n^{(2)}(k_+\rho) + \boldsymbol{N}_n^{(2)}(k_+\rho)\right] + b_n\left[\boldsymbol{M}_n^{(2)}(k_-\rho) - \boldsymbol{N}_n^{(2)}(k_-\rho)\right]\right] \tag{13}$$

$$\vec{H}^s = \frac{j}{\eta}\sum_{n=-\infty}^{\infty} j^n \left[a_n\left[\boldsymbol{M}_n^{(2)}(k_+\rho) + \boldsymbol{N}_n^{(2)}(k_+\rho)\right] - b_n\left[\boldsymbol{M}_n^{(2)}(k_-\rho) - \boldsymbol{N}_n^{(2)}(k_-\rho)\right]\right] \tag{14}$$

where a_n and b_n are the Co and Cross-polarized coefficients respectively. The transmitted fields in region II are given below as

$$\vec{E}^t = \sum_{n=-\infty}^{\infty} j^n \left[c_n\left[\boldsymbol{M}_n^{(3)}(k_1\rho)\right] + d_n\left[\boldsymbol{N}_n^{(2)}(k_1\rho)\right] - e_n\left[\boldsymbol{M}_n^{(3)}(k_2\rho)\right] - f_n\left[\boldsymbol{N}_n^{(2)}(k_2\rho)\right]\right] \tag{15}$$

$$\vec{H}^t = \frac{j}{\eta}\sum_{n=-\infty}^{\infty} j^n \left[c_n\left[\boldsymbol{M}_n^{(3)}(k_1\rho)\right] + d_n\left[\boldsymbol{N}_n^{(2)}(k_1\rho)\right] + e_n\left[\boldsymbol{M}_n^{(3)}(k_2\rho)\right] + f_n\left[\boldsymbol{N}_n^{(2)}(k_2\rho)\right]\right] \tag{16}$$

2.5 Boundary conditions and Bistatic echo width

The boundary conditions are applied to compute the unknown Co and Cross polarized scattering coefficients a_n and b_n respectively. The boundary conditions for chiral-plasma interface at ($\rho = b$) are given as

$$\left.\begin{aligned} \left[\vec{H}^t\right]_{tan} = \left[\vec{H}^i + \vec{H}^s\right]_{tan} \\ \left[\vec{E}^t\right]_{tan} = \left[\vec{E}^i + \vec{E}^s\right]_{tan} \end{aligned}\right\} \tag{17}$$

The subscript "tan" stands for tangential components of the fields. Similarly for plasma-PEMC interface at ($\rho = a$) boundary conditions given in (8) are applied. After the computation of scattering coefficients the normalized bistatic echo widths; ratio of scattered power to incident power, for Co and Cross polarized components are calculated as

$$\left.\begin{aligned} \frac{\sigma_{co}}{\lambda_0} = \frac{2}{\pi}\left|\sum_{n=-\infty}^{\infty} a_n e^{jn(\varphi)}\right|^2 \\ \frac{\sigma_{cross}}{\lambda_0} = \frac{4}{\pi}\left|\sum_{n=-\infty}^{\infty} b_n e^{jn(\varphi)}\right|^2 \end{aligned}\right\} \tag{18}$$

3. Numerical results and discussion

In this section, some numerical results of above formulated scattering theory; electromagnetic scattering from anisotropic plasma coated PEMC cylinder placed in chiral metamaterial, are presented to gain more insight physics and investigations. In all numerical results size of PEMC, PEC and PMC cylinder is taken as $0.7\lambda_0$, thickness of coating is kept as $0.3\lambda_0$ and frequency of incident wave is 1GHz. The host medium i.e., free space, chiral metamaterial, and chiral nihility metamaterial is characterize by the values of parameters i.e., $\varepsilon_c = \varepsilon_0, \mu_c = \mu_0$ & $\beta = 0.0$, $\varepsilon_c = 2.5\,\varepsilon_0, \mu_c = \mu_0$ & $\beta = 0.005$ and $\varepsilon_c = 10^{-2}\,\varepsilon_0, \mu_c = 10^{-2}$ & $\beta = 0.005$ respectively. First of all, the numerical results are compared with published literature [6, 18 & 22] under special conditions as shown in Fig. 2. This comparison ensures the correctness and accuracy of our analytical formulation as well as the functionality of software package (MATHEMATICA).

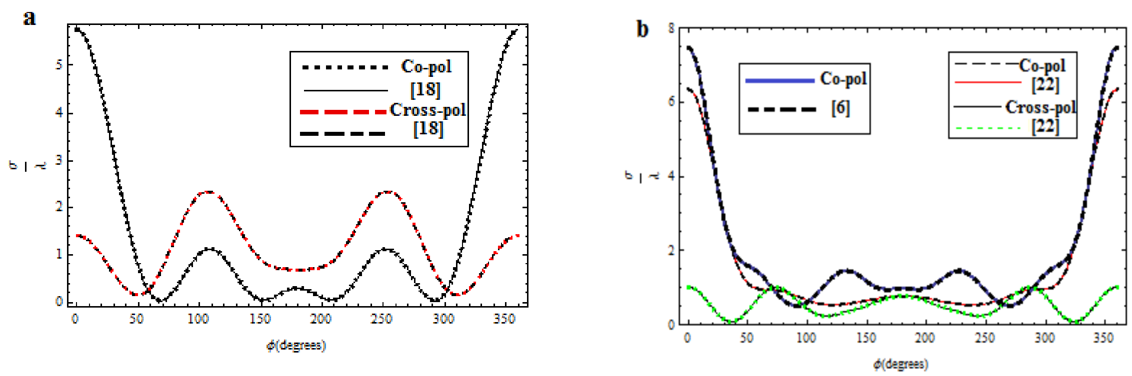

Fig. 2. (a) Comparison between Co-polarized and Cross-polarized bistatic echo widths of anisotropic plasma coated PEMC cylinder. ($b = 10\,cm, f = 1\,GHz, M\eta = \pm 1, \varepsilon_1 = 3.0, \varepsilon_2 = 2j, \varepsilon_3 = 4.0$ and $\mu_r = 1$) (b) Comparison between Co-polarized and Cross - polarized bistatic echo widths of metamaterial coated PEMC cylinder. *($a = 5\,cm, b = 10\,cm, f = 1\,GHz, M\eta = \pm 1, \varepsilon_1 = 3.0, \varepsilon_2 = 2j, \varepsilon_3 = 4.0$ and $\mu_r = 1$).*

Fig. 2(a) shows the comparison between Co and Cross normalized bistatic echowidths of anisiotropic plasma caoted PEMC cylinder. The chiral metamaterial replaced by the free space medium and our problem transfroms into the published literatuer [18]. The Fig. 2(b) shows the comparison between Co and Cross bistatic echowidths of dielectric metamaetrial caoted PEMC cylinder as well as PEC cylinder. The ansiotropic plasma coating is transformed into the isotropic dielectric metamaterial caoting by putting the $\varepsilon_2 = 0$ and $\varepsilon_1 = \varepsilon_3 = 9.8$ and good agreement is found with already avialabel literautre [22]. Then further aproximation $M\eta = \pm\infty$ is applied, the dielectic metamaterial caoetd PEMC cylinder transforms into the dielctric metamaterial caoted PEC cylinder similar to the as in [6].

After the check of accuracy of the work further numerical results are computed for different coated cylinders placed in different host mediums. Fig. 3 shows the Co-polarized and Cross-polarized scattered fields from anisotropic plasma/ dielectric coated perfect cylinders (PEC, PMC & PEMC) placed in free space. Fig. 3(a) shows the comparison of Co-polarized bistatic echo widths of anisotropic plasma, dielectric coated different cylinders in free space. It is obvious from this comparison that plasma coated PEMC cylinder has more stealth capability as compared to other coated cylinders in free space. Fig. 3(b) shows the comparison between the Cross-polarized bistatic echo widths of anisotropic plasma and dielectric coated PEMC cylinders while the PEC and PMC cylinder has no cross polarized fields. The comparison between Co-polarized and Cross polarized bistatic echo widths for anisotropic plasma/ dielectric coated perfect cylinders placed in chiral metamaterial is made as shown in Fig. 4. Fig. 4(a) shows that dielectric coated PEC cylinder has minimum scattering amplitude as compared to other coated cylinders in chiral medium. The cross polarized bistatic echo widths of the same coated cylinders are shown in Fig. 4(b). Fig. 5. Shows the comparison between Co and Cross- polarized bistatic echo widths of differently coated perfect cylinders placed in chiral nihility metamaterial. Fig. 5(a) shows that the scattering amplitude is minimum for anisotropic plasma coated PMC cylinder placed in chiral nihility metamaterial as compared to other coated perfect cylinders in the same host medium. Fig. 5(b) depicts the Cross polarized bistatic echo widths of anisotropic plasma and dielectric coated PEMC cylinder placed in chiral nihility metamaterial.

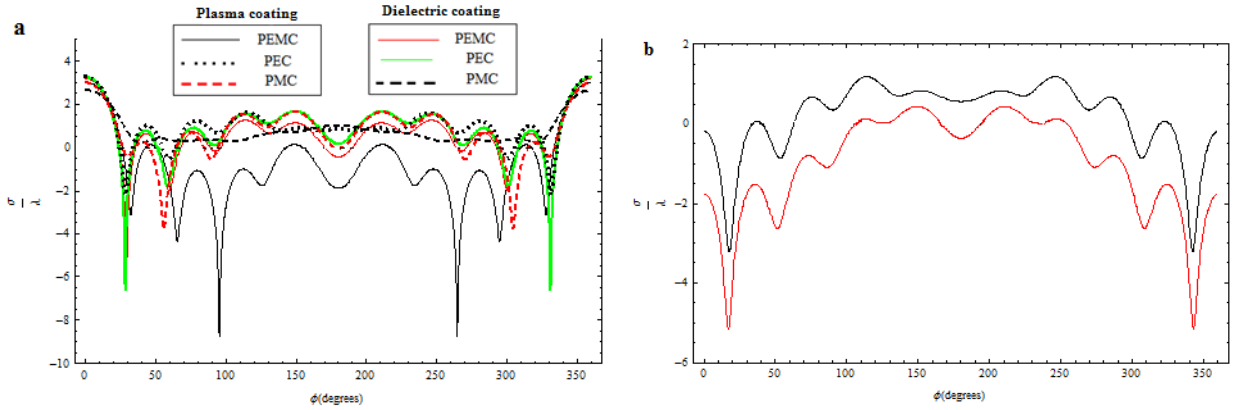

Fig. 3. (a) Co-polarized bistatic echo widths of different coated cylinders placed in free space.(b) Cross-polarized bistatic echo widths of different coated cylinders placed in free space. (Plasma coating: $\varepsilon_1 = 3.0\,, \varepsilon_2 = 2j\,, \varepsilon_3 = 4.0$ *and* $\mu_r = 1$ & *Dielectric coating*: $\varepsilon_1 = \varepsilon_3 = 9.8\,, \varepsilon_2 = 0$).

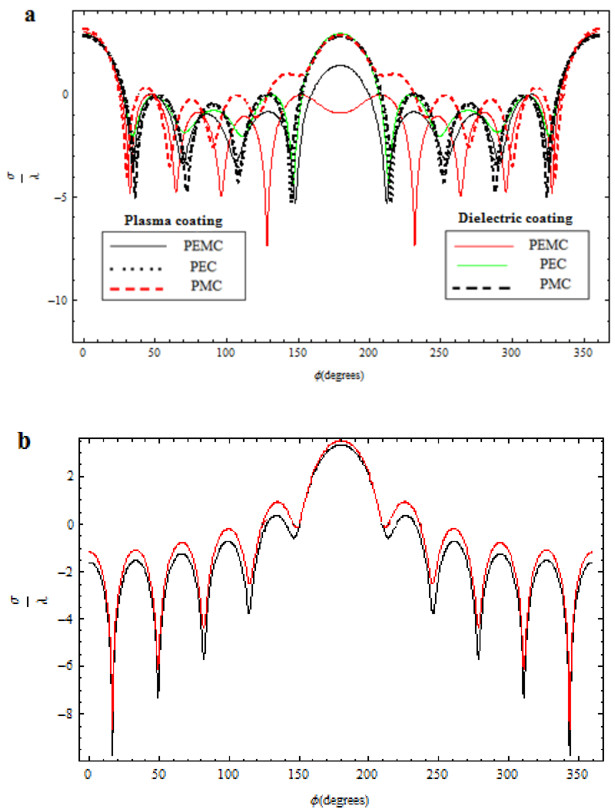

Fig. 4. (a) Co-polarized bistatic echo widths of Different coated cylinders placed in chiral metamaterial. (b) Cross-polarized bistatic echo widths of Different coated cylinders placed in in chiral metamaterial. (*Plasma coating*: $\varepsilon_1 = 3.0\,, \varepsilon_2 = 2j\,, \varepsilon_3 = 4.0$ *and* $\mu_r = 1$ & *Dielectric coating*: $\varepsilon_1 = \varepsilon_3 = 9.8\,, \varepsilon_2 = 0$).

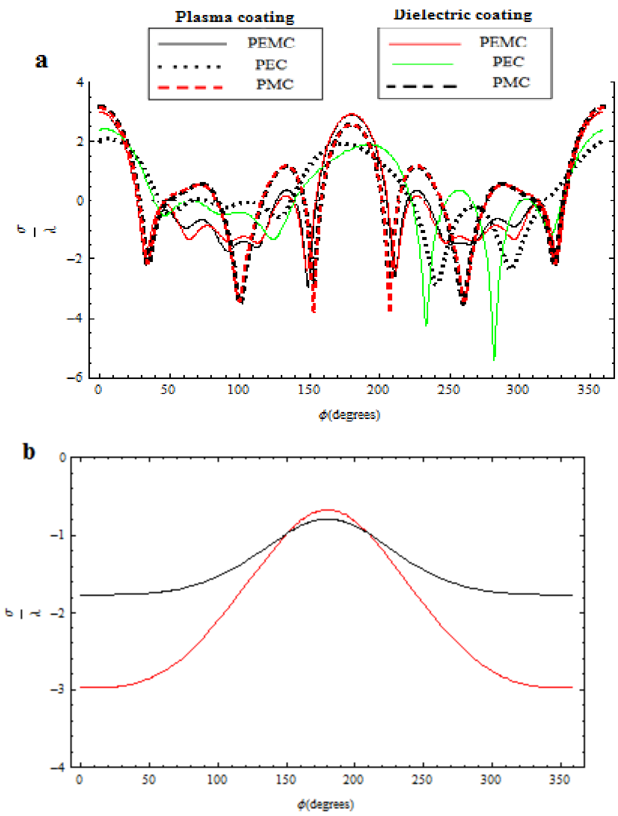

Fig. 5. (a) Co-polarized bistatic echo widths of Different coated cylinders placed in chiral nihility metamaterial. (b) Cross-polarized bistatic echo widths of Different coated cylinders placed in in chiral nihility metamaterial. (*Plasma coating*: $\varepsilon_1 = 3.0\,, \varepsilon_2 = 2j\,, \varepsilon_3 = 4.0$ *and* $\mu_r = 1$ & *Dielectric coating*: $\varepsilon_1 = \varepsilon_3 = 9.8\,, \varepsilon_2 = 0$).

Fig. 6, 7 and 8 shows the comparison between Co polarized bistatic echo widths of different cylinders i.e., PEC, PMC, anisotropic plasma and dielectric placed in free space, chiral metamaterial and chiral nihility metamaterial respectively. The chirality parameter for these results is taken as $\beta = 0.002$. It is very clear from these Figures that metamaterial cylinder has more capability to decrease the radar cross section (RCS) as compared to other type cylinders. Anisotropic plasma and dielectric cylinder almost have the same capability to reduce the RCS in the presence of chiral metamaterial and chiral nihility metamaterials.

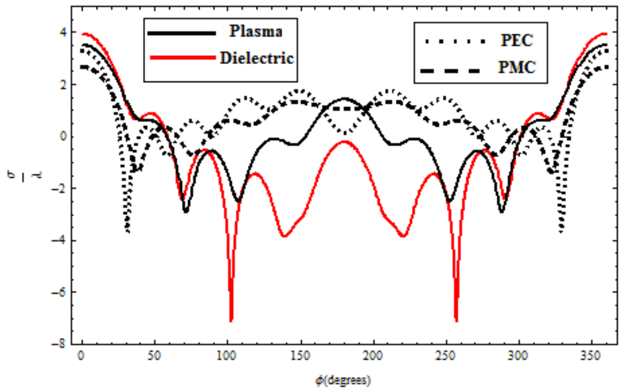

Fig. 6. Comparison between bistatic echo widths of different cylinder placed in chiral metamaterial($a \to 0, b = \lambda_0,\ Plasma\ coating: \varepsilon_1 = 7.0\ , \varepsilon_2 = j\ , \varepsilon_3 = 5.0\ and\ \mu_r = 1, Dielectric\ coating: \varepsilon_1 = \varepsilon_3 = 3.0\ , \varepsilon_2 = 0\ and\ \mu_r = 2.0,\ PEC: \varepsilon_1 = \varepsilon_3 = 10^5\ , \varepsilon_2 = 0\ and \mu_r = 1.0, PMC: \varepsilon_1 = \varepsilon_3 = 1.0\ , \varepsilon_2 = 0\ and \mu_r = 10^5$).

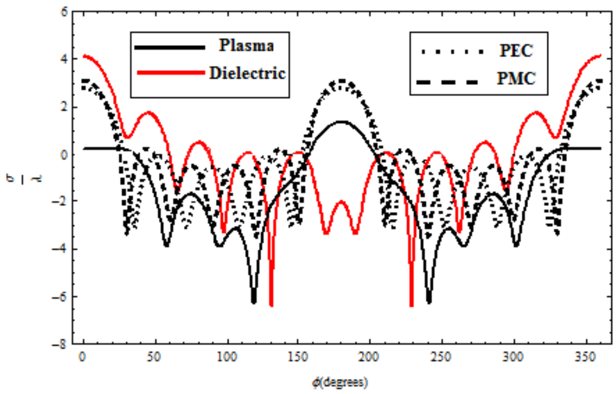

Fig. 7. Comparison between bistatic echo widths of different cylinder placed in chiral metamaterials ($a \to 0, b = \lambda_0,\ Plasma\ coating: \varepsilon_1 = 7.0\ , \varepsilon_2 = j\ , \varepsilon_3 = 5.0\ and\ \mu_r = 1, Dielectric\ coating: \varepsilon_1 = \varepsilon_3 = 3.0\ , \varepsilon_2 = 0\ and\ \mu_r = 2.0,\ PEC: \varepsilon_1 = \varepsilon_3 = 10^5\ , \varepsilon_2 = 0\ and \mu_r = 1.0, PMC: \varepsilon_1 = \varepsilon_3 = 1.0\ , \varepsilon_2 = 0\ and \mu_r = 10^5$).

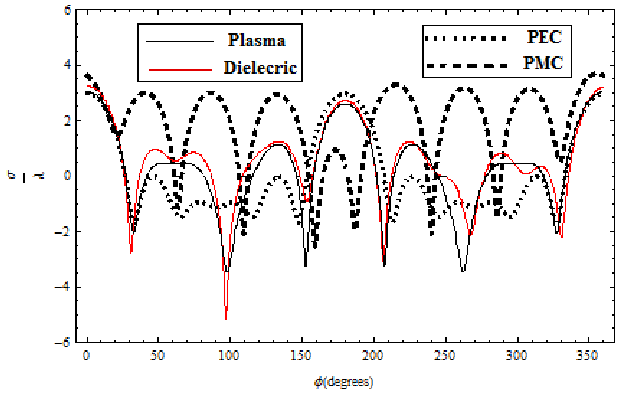

Fig. 8. Comparison of bistatic echo widths of different cylinder placed in chiral nihility metamaterials ($a \to 0, b = \lambda_0,\ Plasma\ coating: \varepsilon_1 = 7.0\ , \varepsilon_2 = j\ , \varepsilon_3 = 5.0\ and\ \mu_r = 1, Dielectric\ coating: \varepsilon_1 = \varepsilon_3 = 3.0\ , \varepsilon_2 = 0\ and\ \mu_r = 2.0,\ PEC: \varepsilon_1 = \varepsilon_3 = 10^5\ , \varepsilon_2 = 0\ and \mu_r = 1.0, PMC: \varepsilon_1 = \varepsilon_3 = 1.0\ , \varepsilon_2 = 0\ and \mu_r = 10^5$).

4. Conclusion

The following conclusions are deduced from the previous section's numeric results:

1) The backward and forward scattering amplitudes can be controlled by the appropriate choice of coating on perfect conductor (PEC, PMC & PEMC) cylinders and as well as by the choice of host medium in which these cylinders are placed.
2) For free space, as a host medium, the anisotropic plasma coated PEMC cylinder helps to reduce the radar cross section (RCS). For chiral and chiral nihility metamaterial, as a host medium, dielectric coated PEC cylinder and anisotropic plasma coated PEMC cylinder has more stealth capability as compared to others radar targets respectively.
3) Regardless the type of host medium is, cross polarized components exist only for PEMC coated cylinders.

Acknowledgment

The authors would like to extend their sincere appreciation to the Deanship of Scientific Research (DSR) at King Saud University for its funding of this research through the Research Group Project noRGP-VPP-312.

References

[1] S. Zhang, Y. S. Park, J. Li, X. Lu, W. Zhang, X. Zhang, Physical review letters, **102**, 023901 (2009).
[2] O. Sakai, K. Tachibana, Plasma Sources Science and Technology, **21**, 013001 (2012).
[3] A. Sihvola, Metamaterials, **1**, 2 (2007).
[4] Z. X. Shan, IEE Proceedings-Microwaves, Antennas

and Propagation, **141**, 279 (1994).
[5] Y. L. Geng, X. B. Wu, L. W Li, B. R. Guan, physical review E, **70**, 056609 (2004)
[6] S. Tretyakov, I. Nefedov, A. Sihvola, S. Maslovski, C. Simovski, Journal of electromagnetic waves and applications, **17**, 695 (2003).
[7] C. Shen, Progress In Electromagnetics Research, **42**, 91 (2003).
[8] D. L, Jaggard, A. R. Mickelson, C. H. Papas, Applied physics, **18**, 211 (1979).
[9] S. Bassiri, C. H. Papas, N. Engheta, JOSA A, **5**, 1450 (1988).
[10] M. A. Al-Kanhal, E. Arvas, Antennas and Propagation, IEEE Transactions on, **44**, 1041 (1996).
[11] S. Shoukat, S. Ahmed, M. A. Ashraf, A. A. Syed, Q. A. Naqvi, Journal of Electromagnetic Waves and Applications, **27**, 1127 (2013).
[12] D. L. Jaggard, J. C. Liu, Journal of electromagnetic waves and applications, **6**, 669 (1992).
[13] S. Ahmed, Q. A. Naqvi, Progress In Electromagnetics Research Letters, **18**, 41 (2010).
[14] S. Shoukat, A. A. Syed, S. Ahmed, Q. A. Naqvi, Optik-International Journal for Light and Electron Optics (2014).
[15] Geng, You-Lin, International Journal of Antennas and Propagation **2011** (2011).
[16] Geng, Youlin, Xinbao Wu, Le-Wei Li, Radio Science **38.6** (2003).
[17] H. Chen, D. Cheng, Antennas and Propagation, IEEE Transactions on **12.3**, 348 (1964).
[18] Yin, Bo, et al. Radiation Effects and Defects in Solids **168.5**, 344 (2013).
[19] A. Ghaffar, M. Z. Yaqoob, Majeed A. S. Alkanhal, M. Sharif, Q. A. Naqvi, AEU-International Journal of Electronics and Communications (2014).
[20] I. V. Lindell, A. H. Shivola, IEEE Transactions on Antennas Propagation, **53**, 3012 (2005).
[21] I. V. Lindell, A. H. Sihvola, IEEE Transactions Antennas Propagation, **54**, 2553 (2006).
[22] R. Ruppin, Journal of Electromagnetic Waves and Applications, **20**, 1853 (2006).
[23] S. Ahmad, Q. A. Naqvi, Optics Communication, **281**, 5664 (2008).
[24] S. Ahmad, Q. A. Naqvi, Progress in Electromagnetics Research, **78**, 25 (2008).
[25] N. Montaseri, M. Soleimani, A. Abdolali, Progress in Electromagnetics Research B, **25**, 173 (2012).

*Corresponding author: zeeshaan32@yahoo.com